Continuous deformation of the Tibetan Plateau from global positioning system data

Pei-Zhen Zhang* State Key Laboratory of Earthquake Dynamics, Institute of Geology, Chinese Earthquake Administration, Beijing 100029, China, and State Key Laboratory of Loess and Quaternary Geology, IEE, CAS, Xi'an, China
Zhengkang Shen State Key Laboratory of Earthquake Dynamics, Institute of Geology, Chinese Earthquake Administration, Beijing 100029, China, and Department of Earth and Space Sciences, University of California, Los Angeles, California 90024, USA
Min Wang, Weijun Gan State Key Laboratory of Earthquake Dynamics, Institute of Geology, Chinese Earthquake Administration, Beijing 100029, China
Roland Bürgmann Department of Earth and Planetary Science, University of California, Berkeley, California 94720, USA
Peter Molnar Department of Geological Sciences, and Cooperative Institute for Research in Environmental Sciences, University of Colorado, Boulder, Colorado 80309, USA
Qi Wang Institute of Seismology, Chinese Earthquake Administration, Wuhan 430071, China
Zhijun Niu, Jianzhong Sun, Jianchun Wu, Sun Hanrong, You Xinzhao National Earthquake Infrastructure Service, Chinese Earthquake Administration, Beijing 100081, China

ABSTRACT

Global positioning system velocities from 553 control points within the Tibetan Plateau and on its margins show that the present-day tectonics in the plateau is best described as deformation of a continuous medium, at least when averaged over distances of >~100 km. Deformation occurs throughout the plateau interior by ESE-WNW extension and slightly slower NNE-SSW shortening. Relative to Eurasia, material within the plateau interior moves roughly eastward with speeds that increase toward the east, and then flows southward around the eastern end of the Himalaya. Crustal thickening on the northeastern and eastern margins of the plateau occurs over a zone ~400 km wide and cannot be the result of elastic strain on a single major thrust fault. Shortening there accommodates much of India's penetration into Eurasia. A description in terms of movements of rigid blocks with elastic strain associated with slip on faults between them cannot match the velocity field.

Keywords: continuous deformation, Tibetan Plateau, flow of crustal material, rigid block, velocity field.

INTRODUCTION

How the Tibetan Plateau deforms in response to the collision of India and Eurasia remains enigmatic and subject to debate; hypotheses have appealed to rigid plates or blocks (e.g., Tapponnier et al., 2001), continuous deformation of the entire lithosphere (Holt et al., 2000; Houseman and England, 1993; Molnar and Tapponnier, 1975), and flow in the lower crust (Royden et al., 1997) to provide keys to the understanding of its mechanism. These different views call for different kinematic descriptions of deformation, but tests using inferences of velocity or strain-rate fields thus far have failed to dissuade proponents of any of these views. If relative movement of rigid blocks can describe regional deformation, we should expect marked velocity gradients near major faults, where interseismic slip deficit accumulates. If instead deformation is continuous, either throughout the lithosphere or by flow in the lower crust, velocity gradients should be relatively smooth.

We synthesized global positioning system (GPS) velocities of 553 control points (see Tables DR1–DR2[1] regarding GPS data processing and synthesis), compared, e.g., to 148 (Wang et al., 2001) and 45 (Chen et al., 2004) points from the same region, in the Tibetan Plateau and along its margins to show in which ways the collision between India and Eurasia is accommodated and to shed new insights on the dynamics of the plateau's contemporary tectonic deformation.

DEFORMATION OF THE TIBETAN PLATEAU

As noted by Wang et al. (2001), GPS velocities indicate that both the NNE-SSW dimension of the Tibetan Plateau and the margins of the plateau, including the Himalaya, the Altyn Tagh, and the Qilian Shan (Figs. 1 and 2), are undergoing horizontal shortening. Rates of convergence between India and the Tarim Basin–Gobi Alashan platform in the direction of relative motion between India and Eurasia (~N20°E) (Sella et al., 2002) are 28.0 ± 2.5, 33 ± 2.0, 34 ± 3.0, and 34 ± 4.0 mm/yr across four parts of the plateau (Fig. 1, profiles D-D′, C-C′, B-B′, and A-A′). These rates account for between 85%–94% (profiles A-A′ and B-B′) and 70%–91% (profiles C-C′ and D-D′) of India's 36–40 mm/yr of convergence with Eurasia (Paul et al., 2001; Shen et al., 2000; Wang et al., 2001), 15–20 mm/yr of it occurring within the Himalaya (Banerjee and Bürgmann, 2002; Larson et al., 1999; Lavé and Avouac, 2000). Shortening across the Tian Shan in the north takes up most of the rest of that convergence.

Within the interior of the plateau, NNW-SSE shortening at 11.3 ± 5.0, 14.0 ± 3.0, and 12.7 ± 3.0 mm/yr along profiles A-A′, B-B′, and C-C′, respectively, and a maximum of 10.0 ± 3.0 mm/yr for D-D′, occurs by smoothly varying rates along the profiles over the entire north-south width of Tibet (Figs. 1 and 3A). These gradients in velocity, therefore, imply distributed deformation of the plateau interior; the long distance of hundreds of kilometers over which the deformation occurs cannot be matched by elastic strain associated with slip at depth on one or two major faults on the edges of or within the plateau.

The NNE-SSW shortening of the plateau interior is accommodated by conjugate strike-slip faulting and orthogonal normal faulting, which do not require that crustal thickening or thrust faulting occur. Neither field investigations (Armijo et al., 1989; Taylor et al., 2003) nor fault-plane solutions of earthquakes (e.g., Molnar and Lyon-Caen, 1989) reveal evidence for active thrust faulting. Instead, they show ESE-WNW extension, which occurs by both normal faulting and conjugate strike-slip fault-

*E-mail: peizhen@ies.ac.cn.

[1]GSA Data Repository item 2004137, Tables DR1–DR3 and Figure DR1, GPS velocities, data processing and synthesis, and velocity profiles, is available online at www.geosociety.org/pubs/ft2004.htm, or on request from editing@geosociety.org or Documents Secretary, GSA, P.O. Box 9140, Boulder, CO 80301-9140, USA.

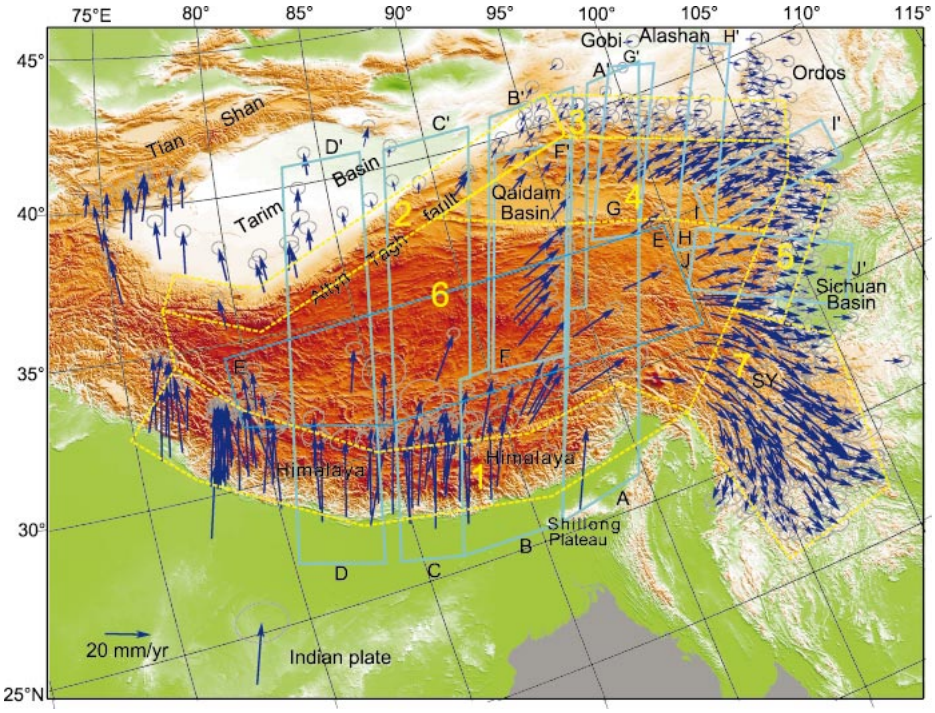

Figure 1. Global positioning system (GPS) velocities (mm/yr) in and around Tibetan Plateau with respect to stable Eurasia, plotted on shaded relief map using oblique Mercator projection. Ellipses denote 1σ errors. Blue polygons show locations of GPS velocity profiles in Figures 3 and DR1 (see footnote 1). Dashed yellow polygons show regions that we used to calculate dilatational strain rates. Yellow numbers 1–7 represent regions of Himalaya, Altyn Tagh, Qilian Shan, Qaidam Basin, Longmen Shan, Tibet, and Sichuan and Yunnan, respectively.

ing. A sum of seismic moment tensors for earthquakes within northern and central Tibet suggests that ESE-WNW extensional strain dominates active deformation of the plateau interior, with approximately half accommodated by strike-slip faulting (NE-trending left lateral and NW-trending right lateral) and half by normal faulting (e.g., Molnar and Lyon-Caen, 1989). GPS data concur with this strain-rate field. Components of velocity parallel to N110°E at stations in the interior of the plateau (Table DR3; see footnote 1) increase eastward to yield eastward stretching of 21.6 ± 2.5 mm/yr between long 79°E and 93°E (Fig. 3B), which is roughly twice the N20°E convergence rate across the plateau interior of 10–14 mm/yr. Simple calculations of strain rate using the velocities of 17 stations located within the plateau interior (Table DR3; see footnote 1) indicate that the average N20°E shortening rates range from $-1.3 \pm 0.4 \times 10^{-8}$ to $-1.8 \pm 0.4 \times 10^{-8}$ yr^{-1}, and the average orthogonal extensional strain rate is $2.1 \pm 0.3 \times 10^{-8}$ yr^{-1}.

The rapid ESE-WNW stretching in the plateau interior results in an eastward movement of crustal material out of India's path. In a reference frame attached to stable Eurasia, ESE velocities not only increase from west to east, but also vary along the profiles, especially A-A′ and B-B′, where measurements span the entire N-S dimension of the plateau. ESE components increase steadily northward from the Himalaya across the breadth of southern Tibet and then decrease farther north across the broad northeastern Tibetan Plateau into the stable Gobi Alashan region (Fig. 3C). Right-lateral shear is difficult to resolve on profile A-A′, but amounts to 10 ± 2 mm/yr on B-B′ in southeastern Tibet between 29°N and 32°N. Left-lateral shear is 12.6 ± 4.4 mm/yr in the northern plateau interior on A-A′ and decreases westward to 9.0 ± 1.5 mm/yr on B-B′. The station spacing and the range of possible interseismic strain-accumulation widths make it difficult to decide how much of the shear is localized on single faults.

Left-lateral shear, ~10–12 mm/yr, is distributed over an ~400-km-wide zone spanning the Kunlun fault (Fig. 3D), a rate consistent with geologically inferred slip rates on

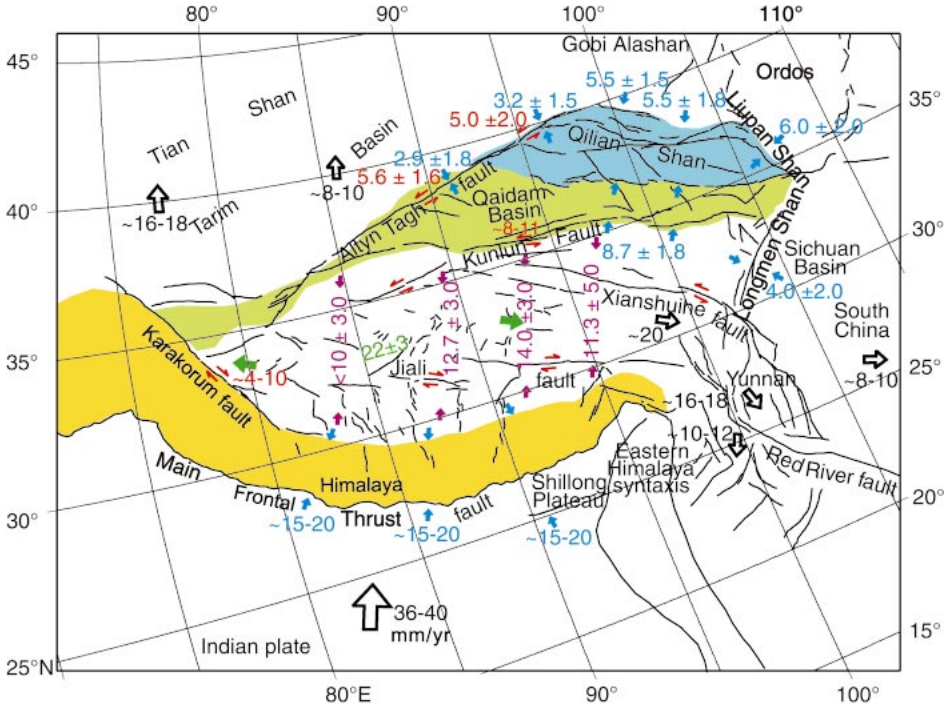

Figure 2. Simplified tectonic map showing active faults and movements of Tibetan Plateau and its margins constrained by global positioning system measurements. Numbers are rates of movement (mm/yr). Map covers same region as Figure 1. Bold black lines show active faults. Bold purple arrows indicate N20°E shortening across interior of plateau. Blue arrows indicate shortening perpendicular to margins of plateau. Green arrows indicate extension in western and central Tibet. Red arrows indicate strike-slip faulting. Open black arrows denote relative motion with respect to stable Eurasia. Colored numbers show respective amounts.

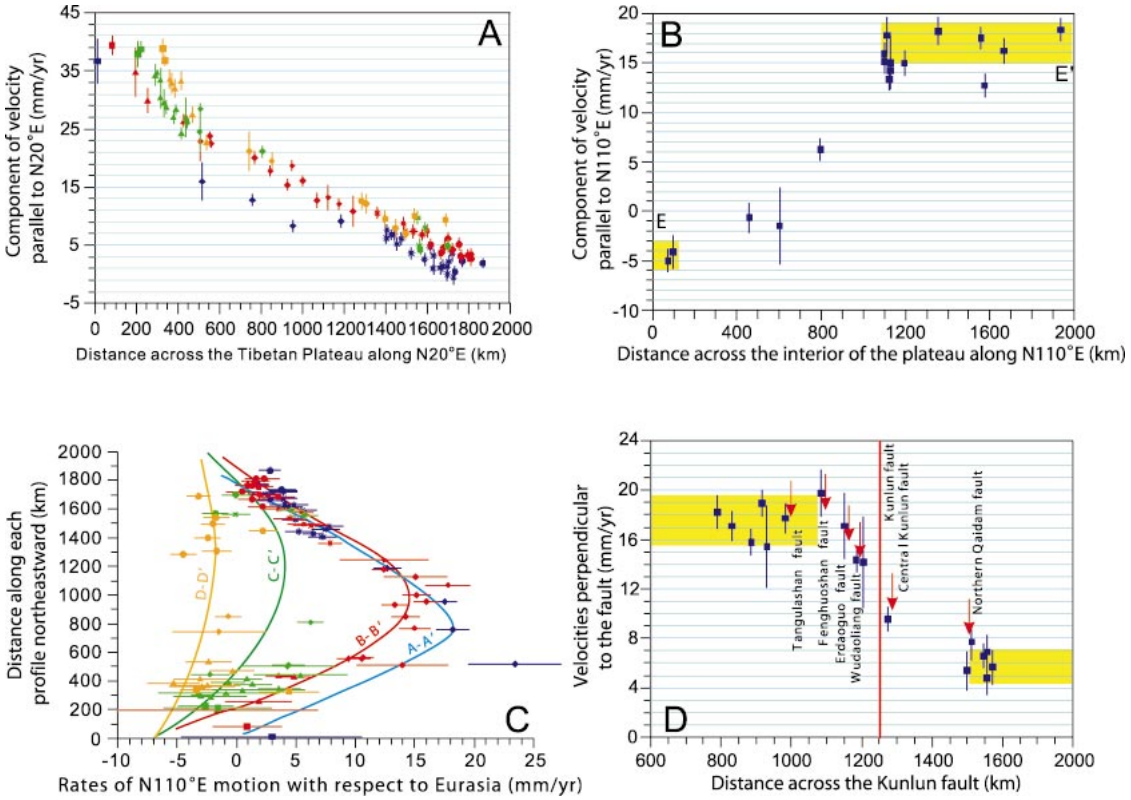

Figure 3. Components velocities of global positioning system (GPS) control points along profiles perpendicular to northeastern and eastern margins of Tibet with respect to stable Eurasia. A: Velocity components parallel to N20°E vs. distance (in km) from south to north (left to right) along each of four profiles in Figure 1. Blue—profile A-A′, red—B-B′, green—C-C′, and orange—D-D′. Squares show GPS stations on Indian plate; triangles—within Himalaya; diamonds—in interior of Tibetan Plateau; stars—in Qaidam and Qilian Shan; dots—in Tarim or Gobi Alashan regions north of Tibetan Plateau. B: Velocity components parallel to N110°E at stations between 31.5°N and 34°N and between 79°E and 100°E (profile E-E′). Yellow bars denote ranges of velocity measurements. C: Velocity components normal to N20°E, inferred India-Eurasia relative motion. Symbols as in A. Curves of different colors sketch approximately eastward flow of each respective profile. D: N10°E trending profile orthogonal to Kunlun fault showing components of east-west motion (profile F-F′, Fig. 1). Yellow bars mark range of measurement (~1 standard deviation). Thick red line marks Kunlun fault. Red arrows denote locations of other active faults within this ~400 km zone.

that fault (Van der Woerd et al., 2000). The inferred rupture depth of 17 km deduced from coseismic GPS data and aftershock locations of a $M_w = 7.8$ earthquake on the Kunlun fault in 2001 (Wang et al., 2003) argue against assignment of this broadly distributed 10–12 mm/yr of shear to elastic strain associated with slip on the Kunlun fault alone (Fig. 3D). Moreover, other active faults have been mapped within the 400-km-wide deformation zone (Figs. 2 and 3D) that might accommodate some of the 10–12 mm/yr of relative movement. In any case, because of the ESE-WNW extension in the region between the shear zones, they cannot bound two rigid blocks; instead, they merely mark zones of more concentrated shear than elsewhere along profiles A-A′ and B-B′.

SHORTENING ON THE NORTHERN AND EASTERN MARGINS

The eastward transfer of crustal material is accommodated by shortening on the margins of the plateau and by clockwise rotation around the eastern Himalayan syntaxis (Figs. 1 and 2). The northern margin of Tibet absorbs only slow convergence: 5.3 ± 1.0 and 6.2 ± 1.5 mm/yr parallel to N20°E on profiles C-C′ and B-B′ (Figs. 1 and 3A), which includes left-lateral strike slip at 5.6 ± 1.6 and 5.0 ± 2.0 mm/yr parallel to the Altyn Tagh fault and 2.9 ± 1.8 and 3.2 ± 1.5 mm/yr of convergence perpendicular to the margin of Tibet (Fig. 2). These strike-slip and convergence rates along the eastern third of the northern plateau margin (profiles B-B′ and C-C′) are consistent with geological (Working Group on the Altyn Tagh Fault [WGATF], 1993) and other geodetic (Bendick et al., 2000; Chen et al., 2001; Shen et al., 2001) results. Shortening occurs at 5.5 ± 1.5 and 5.5 ± 1.8 mm/yr across the northeastern edge of the Tibetan Plateau perpendicular to the western and eastern Qilian Shan, respectively (Figs. DR1A, DR1B; see footnote 1), and 8.7 ± 1.8 mm/yr across the western part of the entire northeastern margin (Fig. DR1A; see footnote 1). In both regions, deformation is spread over zones hundreds of kilometers wide and cannot be associated with elastic strain due to locking near the surface of one or two deep thrust faults. The N15°W-trending Liupan Shan, where folding and thrust faulting take place, forms the easternmost edge of the plateau. A profile perpendicular to the Liupan Shan indicates 6.0 ± 2.0 mm/yr shortening parallel to N75°E (Fig. DR1C; see footnote 1), and the wide distribution of strain suggests that shortening is not localized at the Liupan Shan. The N32°E-trending Longmen Shan with its sharp geomorphic expression marks the east-southeast edge of the plateau margin. As shown by others (Burchfiel et al., 1996; Chen et al., 2001), convergence across the Longmen Shan is relatively slow; we measure only 4.0 ± 2.0 mm/yr oriented N122°E (Fig. DR1D; see footnote 1). In the southeastern margin of the plateau, in the Sichuan-Yunnan region, the Tibetan Plateau gradually grades into the South China block without an obvious topographic boundary, and N-S-trending strike-slip faulting becomes prominent (Figs. 1 and 2). Of the 15–20 mm/yr of east-southeast motion of the interior of Tibet with respect to Eurasia (Figs. 1 and 2), only 8–10 mm/yr is transferred to the South China block.

The flow of Tibetan crustal material surrounding the eastern Himalayan syntaxis, in a reference frame fixed to Eurasia, manifests as movement in a direction oriented clockwise around the syntaxis, including southwestward motion in the western Yunnan province of China, a result consistent with faulting there (e.g., Le Dain et al., 1984; Molnar and Lyon-Caen, 1989; Wang et al., 1998) (Figs. 1 and 2). This kind of rotation differs fundamentally from rigid block rotation, where rates increase away from the rotation axis but remain constant along small circles around the axis of rotation. Neither applies to the velocity field of Figure 1.

DILATATIONAL STRAIN RATES

To test if the surface area changes of the Tibetan Plateau corroborate the kinematic inferences of the deformation described here, we calculated average dilatational strain rates

within regions of homogeneous tectonics (Fig. 1). The negative dilatational strain rate of -4.5×10^{-8} yr^{-1} in the Himalaya indicates areal consumption due to underthrusting of India below southern Tibet. The other margins, such as Altyn Tagh, Qaidam basin and Qilian Shan, Liupan Shan, and Longmen Shan are also subject to areal consumptions with negative dilatational strain rates of -1.1×10^{-8}, -1.1×10^{-8}, -1.1×10^{-8}, and -0.7×10^{-8} yr^{-1}, respectively. Areal expansion is taking place in the plateau interior but with a small positive rate of 0.06×10^{-8} yr^{-1}, consistent with the balance of NNE shortening and ESE extension we describe. The Sichuan and Yunnan region is characterized by areal expansion with a positive rate of 0.7×10^{-8} yr^{-1}, which we interpret as resulting from southeastward and then southward flow of deforming crustal material from the plateau interior around the Himalaya syntaxis. Although uncertainties associated with the strain rate value in each region are tens of percent of the inferred values, due to sparse distribution of GPS stations, the pattern of average dilatational strain confirms the kinematic analysis.

DISCUSSION: RIGID VERSUS VISCOUS DEFORMATION

If a region consisted of a few rigid blocks, each spanning hundreds of kilometers, then strain should be localized near the edges of the blocks. For this case, GPS will have no difficulty demonstrating rigid-block movement by detecting high strain rates across the block edges and low strain rates within the block. Consistent with this view, GPS data surrounding Tibet (Banerjee and Bürgmann, 2002; Paul et al., 2001; Shen et al., 2000; Wang et al., 2001) show low strain rates of $\sim -2.6 \pm 0.9$, -5.0 ± 0.7, 3.9 ± 0.9, and $3.1 \pm 0.6 \times 10^{-9}$ yr^{-1} across the Indian and Alashan platforms and the South China and Ordos blocks, respectively. The much faster strain rate at $1.1 \pm 0.6 \times 10^{-8}$ yr^{-1} across the ~200-km-wide boundary between the Ordos and South China blocks demonstrates strain localization near the edges of the rigid blocks. By contrast, the N20°E shortening rate of $-2.6 \pm 0.2 \times 10^{-8}$ yr^{-1} across the Tibetan Plateau, like the rates on most margins of the plateau, is an order of magnitude greater than the rates in the blocks surrounding the region. Moreover, strain is not localized in zones only ~100–200 km wide along faults within Tibet or on its northeastern and eastern margins, but is spread over distances of 400 km or more.

In addition, most geodetically inferred slip rates corroborate geological estimates of rates ~10 mm/yr along major active strike-slip faults: the Altyn Tagh (Bendick et al., 2000; Shen et al., 2001; WGATF, 1993), Kunlun (Van der Woerd et al., 2000), Karakorum (Banerjee and Bürgmann, 2002; Brown et al., 2002; Jade et al., 2004), and Jiali faults (Armijo et al., 1989; Chen et al., 2004). These rates differ significantly from those envisaged for the plate-like models, which require slip rates of 20–30 mm/yr along the major block-bounding strike-slip faults (e.g., Tapponnier et al., 2001). Whereas deformation in the shallow brittle crust occurs on a distributed network of faults and the neighboring regions may behave as rigid blocks, deformation of a continuous medium at depth best describes the present-day tectonics of the Tibetan Plateau; crustal thickening dominates deformation on its eastern margin, except near the eastern syntaxis of the Himalaya, where rapid clockwise flow around the syntaxis, not rigid-body movement, occurs.

ACKNOWLEDGMENTS

We thank all the global positioning system field crews for collecting the high-quality data that we used for this paper, and Clark Burchfiel and Greg Houseman for thoughtful and constructive reviews. This work has been supported by Ministry of Science and Technology of China, National Science Foundation of China, China Seismological Bureau, and Chinese Academy of Sciences for authors in China. Bürgmann and Molnar acknowledge support from the National Science Foundation (USA).

REFERENCES CITED

Armijo, R., Tapponnier, P., and Han, T., 1989, Late Cenozoic right-lateral strike-slip faulting in southern Tibet: Journal of Geophysical Research, v. 94, p. 2787–2838.

Banerjee, P., and Bürgmann, R., 2002, Convergence across the northwest Himalaya from GPS measurement: Geophysical Research Letters, v. 29, no. 13, doi: 10.1029/2002GL015184.

Bendick, R., Bilham, R., Freymueller, J., Larson, K., and Yin, G., 2000, Geodetic evidence for a low slip rate in the Altyn Tagh fault system: Nature, v. 404, p. 69–72.

Brown, E., Bendick, R., Bourlès, D., Gaur, V., Molnar, P., Raisbeck, G., and Yiou, F., 2002, Slip rates of the Karakorum fault, Ladakh, India, determined using cosmic ray exposure dating of debris flows and moraines: Journal of Geophysical Research, v. 107, no. B9, 2192, doi: 10.1029/2000JB000100.

Burchfiel, B.C., Chen, Z., Liu, Y., and Royden, L., 1996, Tectonics of the Longmen Shan and adjacent regions, Central China: International Geology Review, v. 37, p. 661–735.

Chen, Q., Freymueller, J., Wang, Q., Yang, Z., Xu, C., and Liu, J., 2004, A deforming block model for the present day tectonics of Tibet: Journal of Geophysical Research, v. 109, no. B0, 1403, doi: 10.1029/2002JB002151.

Chen, Z., Burchfiel, B.C., Liu, Y., King, R.E., Royden, L., Tang, W., Wang, E., Zhao, J., and Zhang, X., 2001, Global Positioning System measurements from eastern Tibet and their implications for India/Eurasia intercontinental deformation: Journal of Geophysical Research, v. 105, p. 16,215–16,227.

Holt, W.E., Chamot-Rooke, N., Le Pichon, X., Haines, A.J., Shen-Tu, B., and Ren, J., 2000, Velocity field in Asia inferred from Quaternary fault slip rates and Global Positioning System observations: Journal of Geophysical Research, v. 105, p. 19,185–19,209.

Houseman, G., and England, P., 1993, Crustal thickening versus lateral expulsion in the Indian-Asian continental collision: Journal of Geophysical Research, v. 98, p. 12,233–12,249.

Jade, S., Bhatt, B.C., Bendick, R., Gaur, V.K., Molnar, P., Anand, M.B., and Kumar, D., 2004, GPS measurements from the Ladakh Himalaya, India: Tests of plate-like or continuous deformation in Tibet: Geological Society of America Bulletin (in press).

Larson, K.M., Bürgmann, R., Bilham, R., and Freymueller, J., 1999, Kinematics of the India-Eurasia collision zone from GPS measurements: Journal of Geophysical Research, v. 104, p. 1077–1093.

Lavé, J., and Avouac, J.P., 2000, Active folding of fluvial terraces across the Siwalik hills, Himalayas of central Nepal: Journal of Geophysical Research, v. 105, p. 5735–5770.

Le Dain, A.Y., Tapponnier, P., and Molnar, P., 1984, Active faulting and tectonics of Burma and surrounding regions: Journal of Geophysical Research, v. 89, p. 453–472.

Molnar, P., and Lyon-Caen, H., 1989, Fault plane solutions of earthquakes and active tectonics of the northern and eastern parts of the Tibetan Plateau: Geophysical Journal International, v. 99, p. 123–153.

Molnar, P., and Tapponnier, P., 1975, Cenozoic tectonics of Asia: Effects of a continental collision: Science, v. 189, p. 419–426.

Paul, J., Bürgmann, R., Gaur, V., Bilham, R., Larson, K., Ananda, M., Jade, S., Mukal, M., Anupama, T., Satyal, G., and Kumar, D., 2001, The motion and active deformation of India: Geophysical Research Letters, v. 28, p. 647–650.

Royden, L.H., Burchfiel, B.C., King, R.E., Wang, E., Chen, Z., Shen, F., and Liu, Y., 1997, Surface deformation and lower crustal flow in eastern Tibet: Science, v. 276, p. 788–790.

Sella, G.F., Dixon, T.H., and Mao, A., 2002, REVEL: A model for recent plate velocities from space geodesy: Journal of Geophysical Research, v. 107, no. B4, doi: 10.1029/2000JB000033.

Shen, Z.-K., Zhao, C., Yin, A., Li, Y., Jackson, D., Fang, P., and Dong, D., 2000, Contemporary crustal deformation in East Asia constrained by Global Positioning System measurement: Journal of Geophysical Research, v. 105, p. 5721–5734.

Shen, Z.K., Wang, M., Li, Y., Jackson, D., Yin, A., Dong, D., and Peng, F., 2001, Crustal deformation associated with the Altyn Tagh fault system, western China, from GPS: Journal of Geophysical Research, v. 106, p. 30,607–30,621.

Tapponnier, P., Xu, Z., Roger, E., Meyer, B., Arnaud, N., Wittlinger, G., and Yang, J., 2001, Oblique stepwise rise and growth of the Tibetan Plateau: Science, v. 294, p. 1671–1677.

Taylor, M., Yin, A., Ryerson, F.J., Kapp, P., and Ding, L., 2003, Conjugate strike-slip faulting along the Bangong-Nujiang suture zone accommodates coeval east-west extension and north-south shortening in the interior of the Tibetan Plateau: Tectonics, v. 22, no. 4, doi: 10.1029/2002TC001361.

Van der Woerd, J., Ryerson, F.J., Tapponnier, P., Gaudemer, Y., Finkel, R., Meriaux, S., Caffee, M., Zhao, G., and He, Q., 2000, Uniform slip rate along the Kunlun fault: Implications for seismic behavior and large-scale tectonics: Geophysical Research Letters, v. 27B, p. 2353–2356.

Wang, E., Burchfiel, B.C., Royden, L.H., Chen Liangzhong, Chen Jishen, Li Wenxin, and Chen Zhiliang, 1998, Late Cenozoic Xianshuihe-Xiaojiang, Red River, and Dali fault systems of southwestern Sichuan and central Yunnan, China: Geological Society of America Special Paper 327, 108 p.

Wang, M., Shen, Z.-K., Chen, J., Zhang, Z., Wang, Q., and Gan, W., 2003, Slip distribution of the 2001 Mw 7.8 Kokoxili earthquake, western China: Geophysical Research Abstract, v. 5, abs. 05549.

Wang, Q., Zhang P.-Z., Freymueller, J., Bilham, R., Larson, K., Lai, X., You, X., Niu, Z., Wu, J., Li, Y., Liu, J., Yang, Z., and Chen, Q., 2001, Present-day crustal deformation in China constrained by Global Positioning System (GPS) measurements: Science, v. 294, p. 574–577.

Working Group on the Altyn Tagh Fault, 1993, The Altyn active fault zone: Beijing, China Seismological Press, 319 p.

Manuscript received 12 February 2004
Revised manuscript received 6 May 2004
Manuscript accepted 10 May 2004

Printed in USA